

CONFERENCE ON  
MODELLING FLUID FLOW  
CMFF'09  
SEPTEMBER 9-12, 2009

THE 14<sup>th</sup> EVENT OF INTERNATIONAL CONFERENCE SERIES  
ON FLUID FLOW TECHNOLOGIES HELD IN BUDAPEST

# CONFERENCE PROCEEDINGS

## CD-ROM

Edited by  
J. Vad

Department of Fluid Mechanics  
Budapest University of Technology and Economics

2009

**Proceedings of the Conference on Modelling Fluid Flow  
Budapest University of Technology and Economics, Hungary 2009**

Edited by J. Vad

Copyright © Department of Fluid Mechanics, Budapest University of  
Technology and Economics and the Authors

All Right Reserved

No part of the material protected by this copyright may be reproduced or utilized in any form or by any means, electronic or mechanical, including photocopying, recording or by any storage or retrieve system, without written permission from the copyright owner.

**ISBN 978-963-420-987-4**

Published by Department of Fluid Mechanics  
Budapest University of Technology and Economics  
H-1111 Budapest, Bertalan L. u. 4-6, Hungary  
Tel: +36 1 463 40 72  
Fax: +36 1 463 34 64  
e-mail: vad@ara.bme.hu  
www.ara.bme.hu



# EFFECT OF OSCILLATION AMPLITUDE ON FORCE COEFFICIENTS OF A CYLINDER OSCILLATED IN TRANSVERSE OR IN-LINE DIRECTIONS

László BARANYI<sup>1</sup>, László DARÓCZY<sup>2</sup>

<sup>1</sup> Corresponding Author. Department of Fluid and Heat Engineering, University of Miskolc. Egyetemváros, H-3515 Miskolc, Hungary. Tel.: +36 46 565 154, Fax: +36 46 565 471, E-mail: [arambl@uni-miskolc.hu](mailto:arambl@uni-miskolc.hu)

<sup>2</sup> University of Miskolc, E-mail: [daroczylaszlo@gmail.com](mailto:daroczylaszlo@gmail.com)

## ABSTRACT

A finite difference solution is presented for 2D low Reynolds number flow ( $Re=140$  and  $160$ ) past a circular cylinder placed in a uniform flow. The cylinder is oscillated mechanically either in-line or transversely under lock-in conditions. Abrupt jumps between two state curves were found for a cylinder oscillated in in-line direction in the time-mean (TM) values of lift and torque coefficients when plotted against amplitude of oscillation. Pre- and post-jump analysis carried out included the investigation of phase angle differences, limit cycles and flow patterns confirming the existence of switches in the vortex structure at certain oscillation amplitude values. The TM of drag and base pressure coefficient and the rms values of all force coefficients were continuous functions of oscillation amplitude. When the cylinder was oscillated transversely to the main stream, however, no jumps were found in the corresponding curves. Here the TM of lift and torque were found to be zero (true also for a stationary cylinder) at all amplitude values. Even though the transverse oscillation breaks the symmetry of the flow, there appears to be symmetry over a period.

**Keywords:** CFD, circular cylinder, in-line oscillation, lock-in, low Reynolds number flow, transverse oscillation

## NOMENCLATURE

$A$	[-]	oscillation amplitude, non-dimensionalised by $d$
$C_D$	[-]	drag coefficient, $2D / (\rho U^2 d)$
$C_L$	[-]	lift coefficient, $2L / (\rho U^2 d)$
$D$	[-, N]	dilation or divergence; drag force
$L$	[N]	lift force
$Re$	[-]	Reynolds number, $Ud / \nu$
$St$	[-]	Strouhal number, $f_v d / U$
$T$	[-]	cycle period, non-dimensionalised by $d / U$

$U$	[m/s]	free stream velocity
$a_{0x}, a_{0y}$	[-]	cylinder acceleration in $x$ and $y$ directions, non-dimensionalised by $U^2 / d$
$d$	[m]	cylinder diameter, length scale
$e$	[-]	ellipticity, $A_y / A_x$
$f_v$	[s <sup>-1</sup> ]	vortex shedding frequency
$p$	[-]	pressure, non-dimensionalised by $\rho U^2$
$t$	[-]	time, non-dimensionalised by $d / U$
$tq$	[-]	torque coefficient, torque of shear stress on cylinder surface, non-dimensionalised by $\rho U^2 d^2$
$u, v$	[-]	velocities in $x, y$ directions, non-dimensionalised by $U$
$x, y$	[-]	Cartesian co-ordinates, non-dimensionalised by $d$
$\Delta t$	[-]	time step, non-dimensionalised by $d / U$
$\Theta$	[-]	polar angle characterizing initial condition
$\nu$	[m <sup>2</sup> /s]	kinematic viscosity
$\Phi$	[-]	phase angle
$\rho$	[kg/m <sup>3</sup> ]	fluid density
$\omega$	[-]	vorticity, $\omega = \partial v / \partial x - \partial u / \partial y$ , non-dimensionalised by $U / d$

## Subscripts

D	drag
fb	fixed body
L	lift
mean	time-mean value
rms	root-mean-square value
v	vortex
$x, y$	components in $x$ and $y$ directions
0	for cylinder motion; for stationary cylinder at same $Re$

## 1. INTRODUCTION

The flow around oscillating bluff bodies is an important problem from both academic and practical points of view. Examples are chimneys, silos, transmission lines, or offshore structures –

almost any structure exposed to wind or ocean currents. The near-wake structure of bluff bodies is very rich in complex phenomena in any case, but is especially so when the body is in motion. Transverse oscillation is most often studied, due to its relevance to real-life situations, while in-line oscillation is investigated by fewer researchers. As mentioned in [1] computational experiments benefit from the fact that many of the phenomena observed in flow-induced vibration are weakly dependent on the Reynolds number, and consequently they can be accurately simulated at relatively low Reynolds numbers, as are those in this study.

When vortices are shed periodically from a bluff body, periodic transverse force acting on the body may lead to high amplitude transverse oscillation if the vortex shedding frequency is near to the natural frequency of the body and the damping is small. For a transversely oscillating cylinder, one very important experimental study is that of Williamson and Roshko [2], in which they produced their well-known map of vortex synchronization regions at Reynolds number  $Re=392$ . Forced oscillation studies such as those of Blackburn and Henderson [3] at  $Re=500$  and Kaiktsis et al. [4] at  $Re=200$  found switches in the vortex structure with transverse oscillation around and above the natural vortex shedding frequency ( $St_0$ ). Experimental and numerical investigations have been carried out at  $Re=185$ , identifying switches in vortex structure at around frequency ratio  $f/St_0=1.1$  [5-7].

High-Reynolds number vortex shedding may lead to in-line cylinder oscillation [8]; this led, for instance, to the shutdown of the Monju fast breeder nuclear power plant in 1995. For a cylinder oscillating in in-line direction a fundamental experimental study is [9], investigating the flow over a wide frequency ratio (0.44 to 3) and medium Reynolds number. Al-Mdallal et al. [10] carried out a numerical study at the same wide frequency range but at  $Re=200$ , finding switches in vortex structure only at and over  $f/St_0=1$ . In another numerical study oscillation amplitude was varied at  $Re=1000$  to identify vortex wake modes [8].

Sometimes the body moves in a combination of transverse and in-line oscillation, such as in tube bundles of heat exchangers. Baranyi [11], while investigating the effect of transverse oscillation amplitude of a cylinder on the force coefficients for a cylinder placed in a uniform stream and following an elliptical path (obtained by the superposition of in-line and transverse cylinder oscillations) at low Reynolds number, found switches in the vortex structure. When plotting the TM and rms of force coefficients against transverse oscillation amplitude  $A_y$ , sudden jumps were found in all the TM and rms curves. The number and location of jumps were identical on every curve. There appear to be two states between which the solution switches. The two

state curves can be reached in different ways such as using different ellipticity values [12] or changing the initial position of the cylinder [11]. The solution is attracted to one or the other of two attractors depending on the parameters.

The state curves in [11] fell into two patterns. For the TM of  $C_L$  and  $tq$ , two almost parallel state curves were found. The first point on the curve for the pure in-line ( $A_y=0$ ) case corresponds to one of the two state curves. For the other values, the orbital curves originated from  $A_y=0$  and diverged, and the initial point is naturally identical with the initial point for the pure in-line cases investigated here.

A particular case of orbital motion is that in which the cylinder oscillates in-line, or in transverse direction only. The object of this study is to investigate the effect of oscillation amplitude on these special cases.

## 2. COMPUTATIONAL METHOD

A non-inertial system fixed to the cylinder is used to compute 2D low-Reynolds number unsteady flow around a circular cylinder placed in a uniform stream and forced to oscillate either in transverse or in-line direction. The non-dimensional Navier-Stokes equations for incompressible constant-property Newtonian fluid, the equation of continuity and the Poisson equation for pressure can be written as follows, Eqs. (1) to (4):

$$\frac{\partial u}{\partial t} + u \frac{\partial u}{\partial x} + v \frac{\partial u}{\partial y} = -\frac{\partial p}{\partial x} + \frac{1}{Re} \nabla^2 u - a_{0x} \quad (1)$$

$$\frac{\partial v}{\partial t} + u \frac{\partial v}{\partial x} + v \frac{\partial v}{\partial y} = -\frac{\partial p}{\partial y} + \frac{1}{Re} \nabla^2 v - a_{0y} \quad (2)$$

$$D = \frac{\partial u}{\partial x} + \frac{\partial v}{\partial y} = 0 \quad (3)$$

$$\frac{\partial^2 p}{\partial x^2} + \frac{\partial^2 p}{\partial y^2} = 2 \left[ \frac{\partial u}{\partial x} \frac{\partial v}{\partial y} - \frac{\partial u}{\partial y} \frac{\partial v}{\partial x} \right] - \frac{\partial D}{\partial t} \quad (4)$$

In these equations,  $u$  and  $v$  are the  $x$  and  $y$  components of velocity,  $t$  is time,  $p$  is the pressure,  $Re$  is the Reynolds number based on cylinder diameter  $d$ , free stream velocity  $U$ , and kinematic viscosity  $\nu$ , and  $D$  is the dilation. Although  $D$  is theoretically equal to 0 from Eq. (3), it is kept in Eq. (4) to avoid accumulation of numerical errors.

On the cylinder surface, no-slip boundary condition is used for the velocity and a Neumann type boundary condition is used for the pressure. At the far region, potential flow is assumed.

Boundary-fitted coordinates are used to impose the boundary conditions accurately. Using unique,

single-valued functions, the physical domain bounded by two concentric circles is mapped into a rectangular computational domain with equidistant spacing in both directions (see Figure 1). In the physical domain logarithmically spaced radial cells are used, providing a fine grid scale near the cylinder wall and a coarse grid in the far field. The transformed governing equations and boundary conditions are solved by finite difference method. Space derivatives are approximated by fourth order central differences, except for the convective terms for which a third order modified upwind scheme is used. The Poisson equation for pressure is solved by the successive over-relaxation (SOR) method. The Navier-Stokes equations are integrated explicitly and continuity is satisfied at every time step. For further details see [11, 13].

The 2D code developed by the first author has been extensively tested against experimental and computational results for a stationary cylinder (e.g. [14], see [11]) and computational results for cylinders oscillating in transverse or in in-line directions or following a circular path, including [6, 10, 15], with good agreement being found, [11]. In this study the dimensionless time step is 0.0005, the number of grid points is 361x236, and the physical domain is characterised by  $R_2/R_1=60$ .

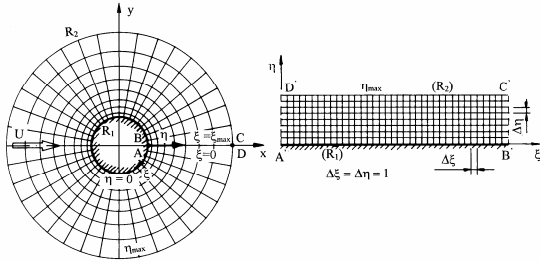


Figure 1. Physical and computational domains

### 3. COMPUTATIONAL SETUP

In this study we investigated the behaviour of flow past a cylinder placed in a uniform stream with its axis perpendicular to the velocity vector of the main flow. The cylinder is oscillated mechanically in either in-line or transverse direction in relation to the uniform stream.

The time-history of force coefficients (lift, drag, base pressure and torque), pressure and velocity field are computed. From these data, time-mean (TM) and root-mean-square (rms) values of force coefficients, streamlines, and vorticity contours can be obtained.

Throughout this paper the lift and drag coefficients used contain the inertial forces originated from the non-inertial system fixed to the accelerating cylinder. Coefficients obtained by removing the inertial forces are often termed ‘fixed body’ coefficients [6]. The relationship between the two sets of coefficients can be written as

$$C_D = C_{Dfb} + \frac{\pi}{2} a_{0x} \quad (5)$$

$$C_L = C_{Lfb} + \frac{\pi}{2} a_{0y}, \quad (6)$$

where subscript ‘fb’ refers to the fixed body (understood in an inertial system fixed to the stationary cylinder), [16]. Since the inertial terms are  $T$ -periodic functions, their time-mean values vanish, resulting in identical TM values for lift and drag in the inertial and non-inertial systems. Naturally the rms values of  $C_L$  and  $C_D$  will be somewhat different in the two systems (but it does not affect the curve being continuous).

For one computation, all parameters are fixed:  $Re$ , frequency ratio, amplitude of oscillation, and initial condition. The computation is then repeated at a different amplitude value, and this is repeated until the amplitude domain over which lock-in holds has been covered. Lock-in, or the synchronisation between vortex shedding and cylinder motion, produces a periodic solution for each of the force coefficients.

For both in-line and transverse oscillation, computations were performed at two Reynolds numbers,  $Re=140$  and  $160$ , holding the frequency ratio  $f/St_0$  constant at 0.9, where  $St_0$  is the non-dimensional vortex shedding frequency from a stationary cylinder at the given Reynolds number. Also, the polar angle  $\Theta=0^\circ$  for initial condition (the cylinder position when starting oscillation: the rightmost position for in-line, the lowest position for transverse oscillation) was held constant. In addition, for in-line oscillation at  $Re=160$ , two further frequency ratios were investigated at  $\Theta=0^\circ$ ,  $f/St_0=0.8$  and  $0.85$ . For  $f/St_0=0.9$ , two further initial conditions were investigated.

### 4. IN-LINE CYLINDER OSCILLATION

The non-dimensional displacement of the centre of the cylinder is described by

$$x_0 = A_x \cos(2\pi f t + \Theta) \quad (7)$$

where  $A_x$  is the amplitude of in-line oscillation,  $f$  is the frequency of cylinder oscillation,  $t$  is the non-dimensional time and  $\Theta$  is the polar angle characterizing the initial condition for the cylinder motion.

#### 4.1. Two patterns

From the TM and rms values of force coefficients plotted against oscillation amplitude, two patterns emerge. One consists of two envelope curves, or state curves, between which the solution jumps (see Figures 2 and 3). This is the pattern found for all TM and rms values in the case of an orbiting cylinder, i.e., transverse and in-line motion

combined [11]. However, for pure in-line oscillation this was true only for the TM of lift  $C_L$  and torque  $tq$ . Here, for the other 6 values – the TM of drag and base pressure and all rms values – a second pattern was identified in which only one curve is found with no sudden jumps in it (see Figure 4). It should be mentioned that for in-line cylinder oscillation lock-in is conventionally considered to be in the vicinity of double the vortex shedding frequency [17]. In this study subharmonic lock-in is considered, near the vortex shedding frequency.

It should be noted that the curves for orbital motion, while all displaying jumps, also fell into two patterns, [11]. For the TM of  $C_L$  and  $tq$ , two almost parallel state curves were found when plotted against the ellipticity of the orbital path ( $e=A_y/A_x$ ). The first point on the curve for the pure in-line ( $A_y=0$ ) case corresponds to one of the two state curves. For the other values, the orbital curves began from one point and diverged, and the initial point is naturally identical with the initial point for the pure in-line cases investigated here.

Lift and torque can be distinguished from the other force coefficients, since they are the only two coefficients for which the location of vortex shedding influences the sign (positive or negative). For these two coefficients, one shedding period includes the shedding of two vortices, one from above the cylinder and one from below (period  $T$ ), whereas with drag and base pressure, one period includes the shedding of one vortex (period  $T/2$ ) and its location has no effect. The rms values are characteristic to the oscillation amplitude of a signal and hence they are independent of the location of the vortex shedding in all cases.

Figures 2 to 4 are for  $Re=160$ ,  $f/St_0=0.8$ ,  $A_y=0$ ,  $\Theta=0^\circ$ , where  $A_x$  is varied across the lock-in domain. As can be seen, Figs. 2 and 3 represent the pattern with two state curves. The number and location of jumps is the same for Fig. 2 and Fig. 3. In each case, the two state curves are mirror images of each other with the axis at  $C_L=0$ . This can be more clearly demonstrated by repeating computations at different initial conditions in order to fill in the gaps in each state curve. Varying  $\Theta$  triggers jumps to the other state curve at different locations; the solution of this non-linear system is highly sensitive to the initial conditions [18]. An example for two initial conditions ( $\Theta=0^\circ$  and  $135^\circ$ ) is shown in Figure 5, for the TM of  $C_L$  at  $f/St_0=0.9$ . The state curves are drawn almost completely with just two initial conditions; the use of further  $\Theta$  values would allow most of the gaps to be filled.

Figure 4 is typical of the second pattern, in which no jumps are found. Curves of this sort were found for the TM values of  $C_{pb}$  and all rms values, as well as for the TM of drag.

Similar results were obtained when the effect of frequency ratio as an independent variable for

values below  $f/St_0=1$  on the force coefficients was investigated, [19]. Only the TM of lift and torque curves contained two different state curves and jumps between them.

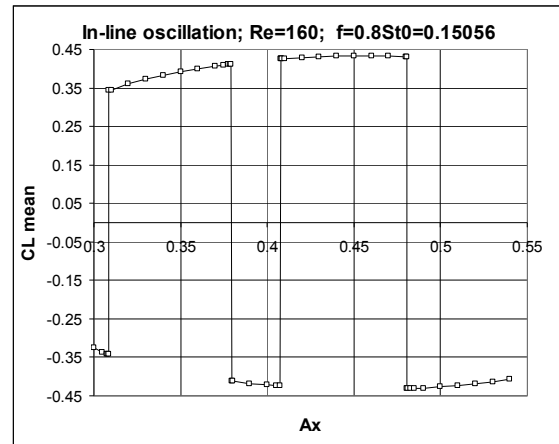


Figure 2. Time-mean value of lift versus amplitude  $A_x$

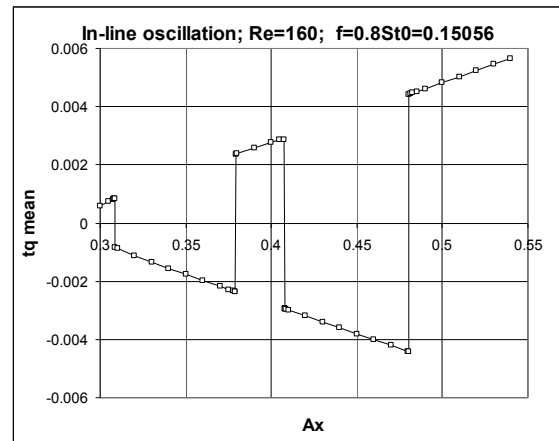


Figure 3. Time-mean value of torque versus amplitude  $A_x$

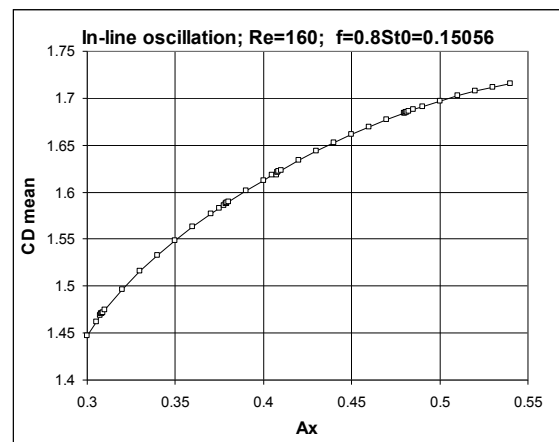


Figure 4. Time-mean value of drag versus amplitude  $A_x$

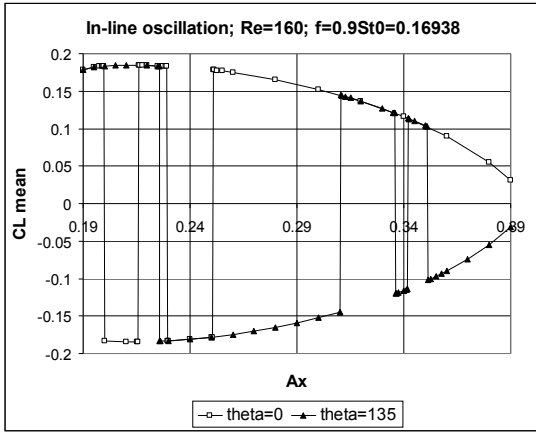


Figure 5. Time-mean value of lift for  $\Theta=0^\circ$  and  $135^\circ$  versus amplitude  $A_x$

#### 4.2. Effect of frequency ratio

As mentioned earlier, computations were carried out for  $Re=160$  at the three frequency ratios  $f/St_0=0.8, 0.85, 0.9$  at the initial condition  $\Theta=0^\circ$ . Figure 6 shows the TM of lift for the three cases. While the lock-in domain shifts, the number and location of jumps vary, and the shape of the curves differs somewhat, it is true in each case that the two state curves are mirror images of each other with respect to  $C_L=0$ . The TM of torque (not shown here) displays similar trends, with the number and location of jumps matching those shown in Fig. 6. For the remaining six cases, naturally no jump occurs, but shifts in the curves occur with varying frequency ratios. Due to lack of space, just the rms of lift is shown, in Figure 7.

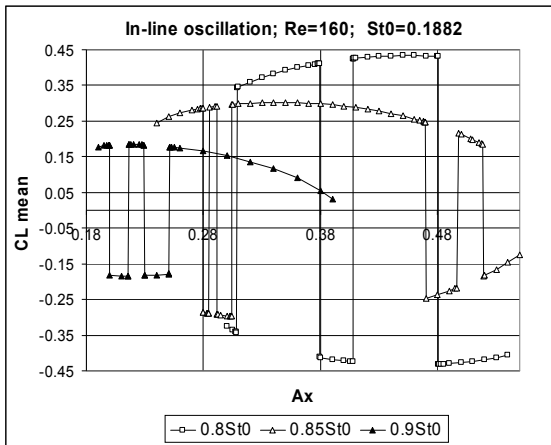


Figure 6. Time-mean value of lift for three frequency ratios versus amplitude  $A_x$

#### 4.3. Pre- and post-jump investigation

Several techniques are used to investigate flow features and whether or how they differ before and after a jump. The particular jump investigated here can be seen in Fig. 5, between  $A_x=0.1997$  (let this be denoted by  $A_{x1}$ ) and  $0.2$  ( $A_{x2}$ ), i.e., the first jump

to occur in the curve for  $\Theta=0^\circ$ . Here,  $Re=160$  and  $f=0.9St_0=0.16938$ .

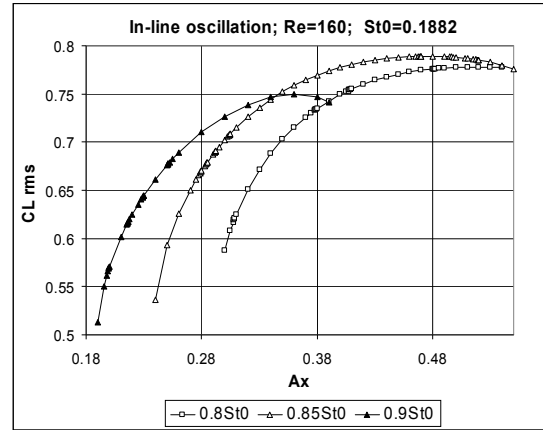


Figure 7. Rms value of lift for three frequency ratios versus amplitude  $A_x$

Time histories of lift and drag are shown in Figures 8 and 9, respectively. In Fig. 8 the thin line shows the time history of lift belonging to amplitude  $A_{x1}$ , while the thick line composed of plus signs belongs to  $A_{x2}$ . The two curves are almost mirror images of each other, meaning a  $\Phi=180^\circ$  phase shift between the two signals. This was confirmed by determining the values of phase angle differences between cylinder displacement (not shown in the figure) and lift. A tiny change in the amplitude value is therefore capable of creating a drastic change in the curve.

For drag, however, the curves for  $A_{x1}$  and  $A_{x2}$  coincide, appearing as if they were one curve (Fig. 9). This shows that drag is not sensitive to the change in amplitude across the critical amplitude value belonging to the jump.

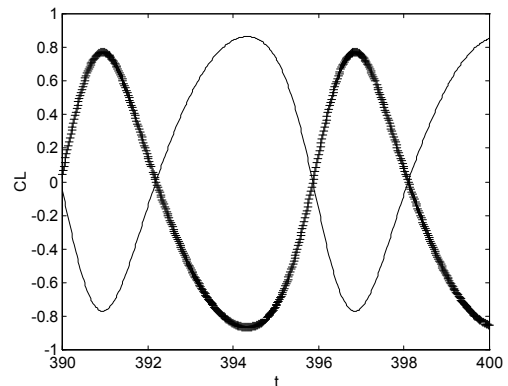
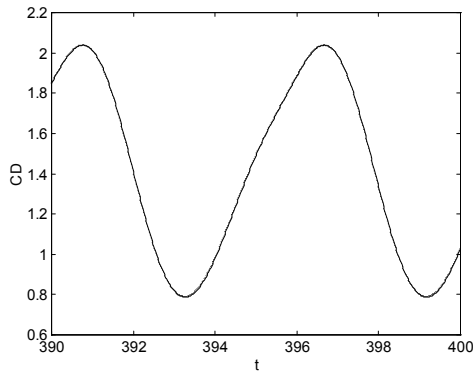


Figure 8. Time history of lift for two  $A_x$  values (thin line:  $A_x=0.1997$ ; thick line:  $A_x=0.2$ ); ( $Re=160, f=0.9St_0, \Theta=0^\circ$ )

Limit cycles (belonging to periodic solutions) were plotted for  $(x_0, C_L)$ ,  $(x_0, C_D)$  and  $(C_D, C_L)$ . Only the last is shown here, in Figure 10. The

dotted line represents the limit cycle for  $A_{x1}$  and the solid line is for  $A_{x2}$ . The arrows show the direction of orientation. Once again, we can see that a very small change in the amplitude results in a radical change, as the limit cycle curves are not only mirror images of each other, but are also opposite in orientation. This finding is similar to that for an orbiting cylinder [11]. Of the other two limit cycles,  $(x_0, C_L)$  showed mirror images for the pre- and post-jump amplitudes, while the two curves  $(x_0, C_D)$  coincided.



**Figure 9.** Time history of drag for two  $A_x$  values (dotted line:  $A_x=0.1997$ ; solid line:  $A_x=0.2$ ); ( $Re=160, f=0.9St_0, \theta=0^\circ$ )

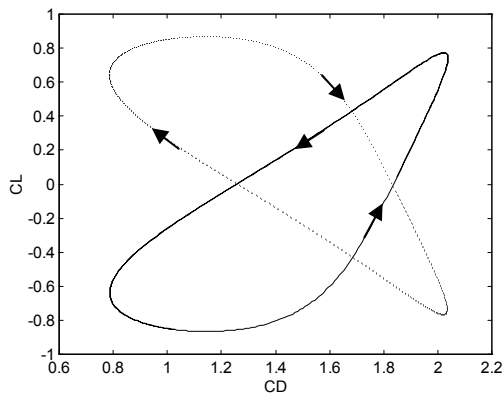


**Figure 10.** Limit cycle ( $C_D, C_L$ ) for two  $A_x$  values (dotted line:  $A_x=0.1997$ ; solid line:  $A_x=0.2$ ); ( $Re=160, f=0.9St_0, \theta=0^\circ$ )

Vorticity contours are shown in Figure 11. Contours of positive (black) and negative (grey) vorticity  $\omega$  are shown for pre-jump (a) and post-jump (b) amplitudes. Contours shown belong to the uppermost cylinder position. As seen in the figure, the flow patterns are essentially mirror images of each other. Note that the vortex shedding pattern is mode P, in which one pair of vortices is shed in a complete cycle [2].

All results of the pre- and post-jump investigation support the idea that there are two solutions of this non-linear system. Whether the actual solution is attracted to one solution, or

attractor, or to the other depends on the parameters. It is clear that a tiny change in a parameter – amplitude, in this case – can be enough to lead to a switch in attractors. The boundary between the basins of attraction seems to be quite distinct.

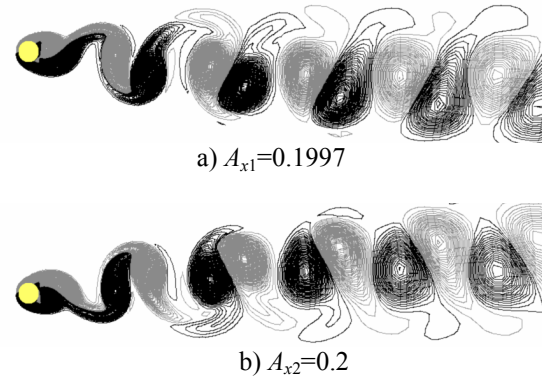


**Figure 11.** Vorticity contours for a cylinder oscillating in-line at uppermost cylinder position ( $Re=160, f=0.9St_0, \theta=0^\circ$ )

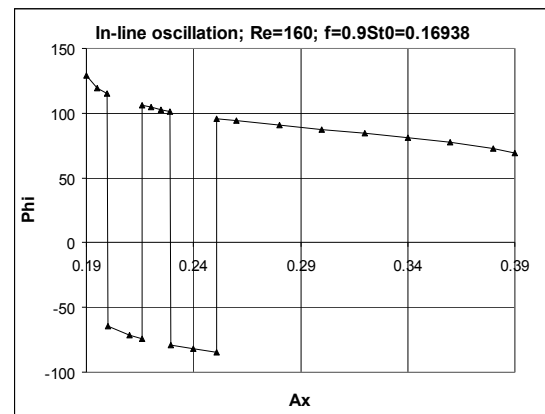


**Figure 12.** Phase angle between lift and cylinder displacement vs.  $A_x$  ( $Re=160, f=0.9St_0, \theta=0^\circ$ )

## 5. TRANSVERSE CYLINDER OSCILLATION

Flow past a cylinder was also investigated when the cylinder was oscillated transversely to the main stream. The non-dimensional displacement of the centre of the cylinder is described by

$$y_0 = -A_y \sin(2\pi f t + \Theta) \quad (8)$$

Systematic computations were carried out for a transversely oscillated cylinder for two sets of parameters, ( $Re=140; f=0.9St_0=0.16389; \theta=0^\circ$ ) and ( $Re=160; f=0.9St_0=0.16938; \theta=0^\circ$ ) over the amplitude domain where lock-in condition prevailed. Plotting TM and rms values against  $A_y$  gave only continuous curves; no jumps were found at all in any of the force coefficients.

Another important finding for the transversely oscillating cylinder is that the TM value of lift and

torque are zero for all oscillation amplitude values investigated:

$$C_{L\text{mean}} = t q_{\text{mean}} = 0 \quad (9)$$

It seems that although instantaneously the symmetry is broken by the transverse oscillation, over a vortex shedding period there is symmetry.

Figures 13 and 14 show two examples for transversely oscillating cylinders for the two Reynolds numbers investigated. Fig. 13 shows the rms of lift, Fig. 14 the TM of drag against oscillation amplitude  $A_y$ . No jumps can be detected in the curves and the relatively small change in  $Re$  does not have a dramatic effect on the curves, the effect being smaller for the TM of drag (Fig. 14).

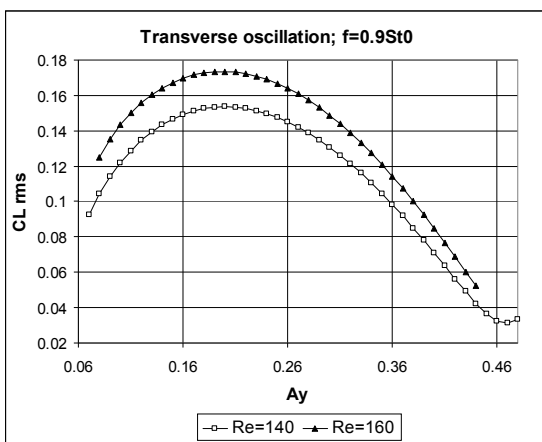


Figure 13. Rms value of lift versus amplitude  $A_y$  for  $Re=140$  and  $160$

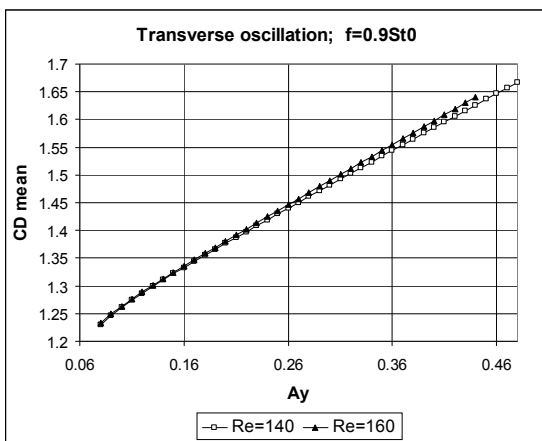


Figure 14. Time-mean value of drag versus amplitude  $A_y$  for  $Re=140$  and  $160$

Figure 15 shows the vorticity contours for a transversely oscillating cylinder. The flow structure is 2S, i.e., two single vortices are shed in one cycle [2], giving the well-known Kármán vortex street.

Obtained results for transversely oscillating cylinder do not contradict published results.

Researchers have investigated the effect of frequency ratio on the flow. In [3] at  $Re=500$  and  $A_y=0.25$  switches were found in the vortex structure between the frequency ratios of 0.875 and 0.975. Other studies never found switches in vortex structure below frequency ratio 1, e.g. in [4] the critical  $f/St_0$  is  $\geq 1$  at  $Re=200$ , and in [5-7] it is between 1.1-1.12 at  $Re=185$ .

Similar results were obtained when the effect of frequency ratio as an independent variable for values below  $f/St_0=1$  on the force coefficients was investigated for a transversely oscillated cylinder, [19]. None of the TM and rms of force coefficients contained jumps.

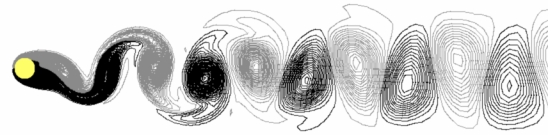


Figure 15. Vorticity contours for a cylinder oscillating transversely ( $Re=160$ ;  $A_y=0.2$ ;  $f=0.9St_0=0.16938$ )

## 6. CONCLUSIONS

The effect of oscillation amplitude on the time-mean and rms values of force coefficients when plotted against amplitude was investigated for a cylinder oscillating either in transverse or in-line direction under lock-in condition. The investigated cases included Reynolds numbers  $Re=140$  and  $160$ , frequency ratios of  $f/St_0=0.8$ ,  $0.85$  and  $0.9$ , and three different initial conditions for the cylinder motion.

For *in-line cylinder oscillation*, jumps were found in the TM values of lift and torque coefficients when plotted against oscillation amplitude. There are two state curves and the solution jumps between them. The number and location of jumps are identical for the two TM curves. State curves are mirror images of each others. The state curves can be fully realised by using different initial conditions.

Pre- and post-jump investigations (time history, limit cycle, vorticity contours) confirmed switches in the vortex structure. Time history of lift and vorticity contours are almost mirror images of each other for pre- and post-jump amplitude values. The phase angle difference between cylinder displacement and lift undergoes a  $180^\circ$  switch through a jump. Vorticity contours show that a pair of vortices (P, see [2]) is shed in each cycle.

For lift and torque coefficients, one shedding period includes the shedding of two vortices, one from above the cylinder and one from below (period  $T$ ), whereas with drag and base pressure, one period includes the shedding of one vortex (period  $T/2$ ) and its location has no effect. Only lift and torque depend on where the vortex is shed from and can thus have either positive or negative values.

The rms values are characteristic to the oscillation amplitude of a signal and are hence independent of the location of the vortex shedding. No jumps were detected for the TM of drag or base pressure, or for the rms of any of the four coefficients.

For *transverse cylinder oscillation*, no jumps were found in any TM or rms curves for the set of parameters investigated. The TM value of lift and of torque was zero (as for a stationary cylinder) for all amplitudes investigated. Vorticity contour plots reveal 2S shedding (two single vortices are shed in a cycle), or the Kármán vortex street [2].

Although one would expect that the symmetry would be broken for the transversely oscillating cylinder, still it seems that symmetry is maintained over a cycle. Somewhat surprisingly, it is the in-line oscillation case in which the sudden switches in vortex structure occur. This requires further investigation. Additionally, investigations over a wider parameter range are planned.

## ACKNOWLEDGEMENTS

This work has been supported by the Hungarian National Fund for Science and Research under contract No. OTKA K 76085.

## REFERENCES

- [1] Newman, D.J., and Karniadakis, G.E., 1995, "Direct numerical simulations of flow over a flexible cable", *Proc. 6th Int. Conference on Flow-Induced Vibration*, London, pp. 193-203.
- [2] Williamson, C.H.K., and Roshko, A., 1988, "Vortex formation in the wake of an oscillating cylinder", *Journal of Fluids and Structures*, Vol. 2, pp. 355-381.
- [3] Blackburn, H.M., and Henderson, R.D., 1999, "A study of two-dimensional flow past an oscillating cylinder", *Journal of Fluid Mechanics*, Vol. 385, pp. 255-286.
- [4] Kaiktsis, L., Triantafyllou, G.S., and Özbas, M., 2007, "Excitation, inertia, and drag forces on a cylinder vibrating transversely to a steady flow", *Journal of Fluids and Structures*, Vol. 23, pp. 1-21.
- [5] Gu, W., Chyu, C., and Rockwell, D., 1994, "Timing of vortex formation from an oscillating cylinder", *Physics of Fluids*, Vol. 6, pp. 3677-3682.
- [6] Lu, X.Y., and Dalton, C., 1996, "Calculation of the timing of vortex formation from an oscillating cylinder", *Journal of Fluids and Structures*, Vol. 10, pp. 527-541.
- [7] Guilmineau, E., and Queutey P., 2002, "A numerical simulation of vortex shedding from an oscillating circular cylinder", *Journal of Fluids and Structures*, Vol. 16, pp. 773-794.
- [8] Rodriguez, M., and Mureithi, N.W., 2006, "Cylinder wake dynamics in the presence of stream-wise harmonic forcing", *Proc. PVP2006-ICPVT-11*, Vancouver, Canada, on CD ROM, pp. 1-9.
- [9] Cetiner, O., and Rockwell, D., 2001, "Streamwise oscillations of a cylinder in a steady current. Part 1. Locked-on states of vortex formation and loading", *Journal of Fluid Mechanics*, Vol. 427, pp. 1-28.
- [10] Al-Mdallal, Q.M., Lawrence, K.P., and Kocabiyik, S., 2007, "Forced streamwise oscillations of a circular cylinder: Locked-on modes and resulting fluid forces", *Journal of Fluids and Structures*, Vol. 23, pp. 681-701.
- [11] Baranyi, L., 2008, "Numerical simulation of flow around an orbiting cylinder at different ellipticity values", *Journal of Fluids and Structures*, Vol. 24, pp. 883-906.
- [12] Baranyi, L., 2004, "Numerical simulation of flow past a cylinder in orbital motion", *Journal of Computational and Applied Mechanics*, Vol. 5, pp. 209-222.
- [13] Baranyi, L., 2003, "Computation of unsteady momentum and heat transfer from a fixed circular cylinder in laminar flow", *Journal of Computational and Applied Mechanics*, Vol. 4, pp. 13-25.
- [14] Chakraborty, J., Verma, N., and Chhabra, R.P., 2004, "Wall effects in flow past a circular cylinder in a plane channel: a numerical study", *Chemical Engineering and Processing*, Vol. 43, pp. 1529-1537.
- [15] Didier, E., and Borges, A.R.J., 2007, "Numerical predictions of low Reynolds number flow over an oscillating circular cylinder", *Journal of Computational and Applied Mechanics*, Vol. 8, pp. 39-55.
- [16] Baranyi, L., 2005, "Lift and drag evaluation in translating and rotating non-inertial systems", *Journal of Fluids and Structures*, Vol. 20, pp. 25-34.
- [17] Griffin, O.M., and Hall, M.S., 1991, "Review—Vortex shedding lock-on and flow control in bluff body wakes", *Journal of Fluids Engineering, Trans. ASME*, Vol. 113, pp. 526-537.
- [18] Strogatz, S.H., 1994, *Nonlinear Dynamics and Chaos*, Addison-Wesley Publishing Company.
- [19] Baranyi, L., 2008, "Effect of frequency ratio on the force coefficients of a cylinder oscillated in a uniform stream", *Proc. 7th JSME-KSME Thermal and Fluids Engineering Conference*, Sapporo, Japan, on CD ROM, paper L132, pp.1-4.